Mech. Sci., 6, 51–55, 2015
www.mech-sci.net/6/51/2015/
doi:10.5194/ms-6-51-2015

Mechanical Sciences
Open Access

Friction Stir Welding of AA2024-T3 plate – the influence of different pin types

D. Trimble, H. Mitrogiannopoulos, G. E. O'Donnell, and S. McFadden

Department of Mechanical and Manufacturing Engineering, Trinity College Dublin, Dublin 2, Ireland

Correspondence to: S. McFadden (shaun.mcfadden@tcd.ie)

Received: 30 January 2015 – Revised: 24 March 2015 – Accepted: 31 March 2015 – Published: 17 April 2015

Abstract. Some aluminium alloys are difficult to join using traditional fusion (melting and solidification) welding techniques. Friction Stir Welding (FSW) is a solid-state welding technique that can join two plates of material without melting the workpiece material. This proecess uses a rotating tool to create the joint and it can be applied to alumium alloys in particular. Macrostructure, microstructure and micro hardness of friction stir welded AA2024-T3 joints were studied. The influence of tool pin profile on the microstructure and hardness of these joints was examined. Square, triflute and tapered cylinder pins were used and results from each weldment are reported. Vickers micro hardness tests and grain size measurements were taken from the transverse plane of welded samples. Distinct zones in the macrostructure were evident. The zones were identified by transitions in the microstructure and hardness of weld samples. The zones identified across the sample were the the unaffected parent metal, the Heat Affected Zone (HAZ), the Thermo-Mechanicaly Affected Zone (TMAZ), and the Nugget Zone (NZ). Measured hardness values varied through each FSW zone. The hardness in each zone was below that of the parent material. The HAZ had the lowest hardness across the weld profile for each pin type tested. The cylindrical pin consistently produced tunnel and joint-line defects. Pin profiles with flat surface features and/or flutes produced consolidated joints with no defects.

1 Introduction

The Welding Institute (TWI) developed Friction Stir Welding (FSW) in 1991 (Thomas, 1991) and it is considered to be one of the most significant developments in metal joining in recent times. It is a solid-state welding technique used for joining aluminium alloys (as shown in Fig. 1). This technique is currently being applied in the aerospace, automotive, and shipbuilding industries (Mishra and Ma, 2005) and was recently reviewed in Xiaocong et al. (2014).

Due to its solid state nature FSW has many benefits over fusion welding techniques. However, one of its main advantages is its ability to weld all series of aluminium alloys, in particular the 2xxx series alloys (Yang et al., 2008; Trimble et al., 2012). These alloys are used extensively within the aerospace industry for applications such as fuselage and wing skin panels due to their high strength-to-weight ratio. However, these alloys are mostly non-weldable using fusion welding methods due to problems with oxidisation, solidification, shrinkage, sensitivity to cracking, hydrogen solubility and the resultant porosity problems (Flores et al., 1998).

FSW involves the translation of a tool along the joint line between two plates. The tool rotates at high speeds during the process. The tool is made up of a profiled pin and a shoulder which generate frictional heat to soften the workpiece material either side of the joint line and mix the workpiece materials together. The FSW tool is not consumed in the process and is crucial to the welding process. The shoulder generates the largest component of heat in the process. The pin causes localised heating and plastic deformation of the material around the pin.

The macrostructure of a FSW joint consists of three distinct zones; the central Nugget Zone (NZ), the Thermomechanically Affected Zone (TMAZ) and the Heat Affected Zone (HAZ). The zonal microstructure of a FSW joint is shown in Figs. 1 and 2. The objective of this work was to determine the variation in hardness across a FSW joint and determine the correlation between microstructure and hard-

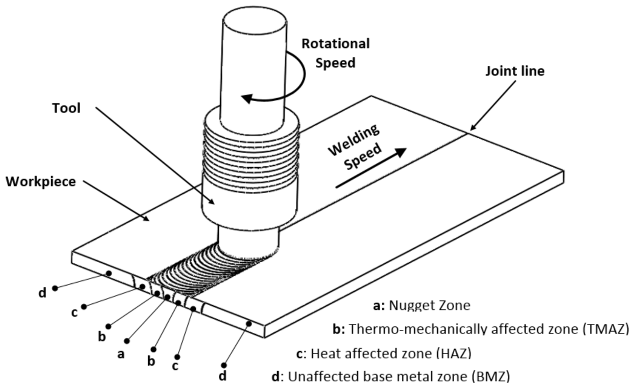

Figure 1. Friction Stir Welding (FSW) schematic.

Figure 2. Zonal macrostructure of AA2024-T3 after FSW.

ness. The effect of pin profile on the microstructure and hardness of FSW joints was examined.

2 Experiemtal procedure

A Corea F3UE vertical milling machine was modified for use in this experiment. Figure 3 gives details of the FSW tooling. Aluminium alloy AA2024-T3 plates (4.8 mm thick) were butt welded using three different pin profiles: tapered cylinder, square and triflute. All pins were 4.6 mm in length. The swept diameter of the square pin was 7 mm. The swept diameter of the tapered cylinder and triflute pins tapered from 7 mm (at the shoulder) to 2.69 mm. A scrolled shoulder was used in this investigation (no tilt angle was required). Rotational and translational speeds were 450 rpm and 180 mm min^{-1}, respectively.

Samples were cut from the cross-section of each FSW joint and prepared for post weld analysis. Samples were polished to remove all tool marks and scratches. The samples were then etched using Keller's reagent to reveal the microstructure. Samples were viewed using a Leica DM LM microscope and ImageJ software was used to measure grain size. Vickers microhardness tests were carried out using a Mitutoyo MVK-H1 micro hardness machine. Four rows and twenty five columns of indents were made across the weld samples with 1 mm horizontal spacing maintained between columns. The indent rows were positioned 1, 2, 3.25 and 4.5 mm from the base of the sample.

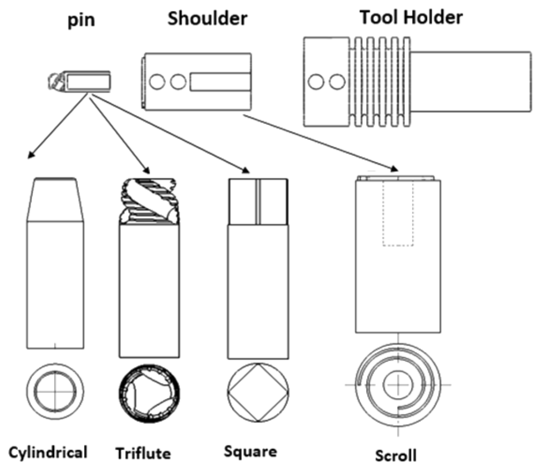

Figure 3. The tooling used including three pin profiles, the scroll shoulder, and tool holder.

3 Results and discussion

Microstructural analysis revealed a complex microstructure in the FSW zone. On a macrostructural level the weld zone was found to be trapezoidal in shape for each pin. Figure 4 shows the results of macrostructural analysis for the three pin profiles. By comparing the swept diameter of each pin to the width of the nugget zone for each pin it is clear that tool geometry is directly linked to the shape of the FSW zone. Despite having the same swept diameter, it can be seen that the NZ of the triflute pin does not narrow with depth from the workpiece surface as drastically as that of the tapered cylinder pin. This was due to increased mixing action resulting from the flutes in the pin surface. The greater mixing action of the square and triflute pins resulted in a larger NZ when compared to the tapered cylinder pin.

A tunnel defect (an internal void) was observed in the welds performed by the tapered cylinder pin. This defect, shown in Fig. 5, was observed in the transition region between the NZ and the TMAZ at a depth similar to the plunge depth of the pin and on one side only. This is because the cylindrical pin produces less plastic deformation and stirring of the workpiece. Insufficient plastic flow around the pin gave rise to the conditions for the formation of the tunnel defect.

Another defect that was consistently found in the joint made with the tapered cylinder pin was a joint line remnant (Fig. 6). This feature is located at the original position of the joint interfaces at the bottom of the welded joint. Again, this feature is symptomatic of the insufficient plastic deformation and stirring of the metal when the tapered cylinder pin is used.

The HAZ, TMAZ and NZ were defined by different microstructural features. Figure 7 shows examples of the typical grain structures found in the distinct zones. Figure 7a shows the microstructure of the parent material. This microstructure

Pin Profile	Macrostructure	Size of Nugget Zone (mm) W	Size of Nugget Zone (mm) H	Shape of FSW Zone	Defects
Tapered Cylinder		13.40 4.59 2.64	4.8	Trapezoidal	1. Tunnel defect at plunge depth of pin. 2. Remnants of joint line at base
Square		13.67 7.37 5.51	4.8	Trapezoidal	None
Triflute		13.01 5.72 3.57	4.8	Trapezoidal	None

Figure 4. Macrostructural data for three pin profiles.

Table 1. Variation in grain size in the nugget zone.

Pin type	Location in Nugget zone	Min.	Max.	Range	Avg.
		Grain sizes (µm)			
Square	Top	1.60	3.47	1.87	2.23
	Right of Centre	1.60	4.29	2.69	2.20
	Centre	1.62	3.42	1.80	2.24
	Left of Centre	1.64	3.42	1.78	2.09
	Bottom	1.60	3.50	1.90	2.16
Tapered cylinder	Top	1.61	3.66	2.05	2.17
	Right of Centre	1.61	5.00	3.39	2.46
	Centre	1.60	4.00	2.40	2.18
	Left of Centre	1.64	5.43	3.79	2.43
	Bottom	1.60	3.36	1.76	2.24
Triflute	Top	1.60	3.36	1.76	2.23
	Right of Centre	–	–	–	–
	Centre	1.60	3.46	1.86	2.17
	Left of Centre	1.60	5.01	3.41	2.35
	Bottom	1.61	3.85	2.24	2.17

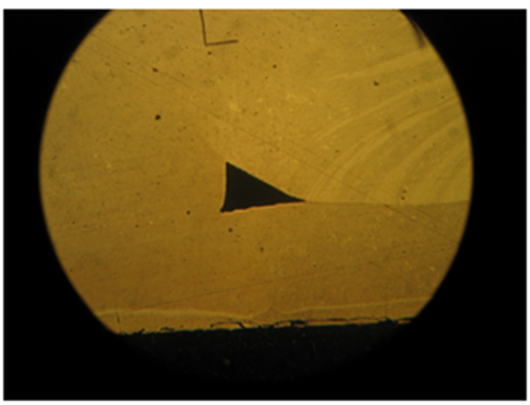

Figure 5. Tunnel defect found in the tapered cylinder FSW joint ($\times$ 50 magnification).

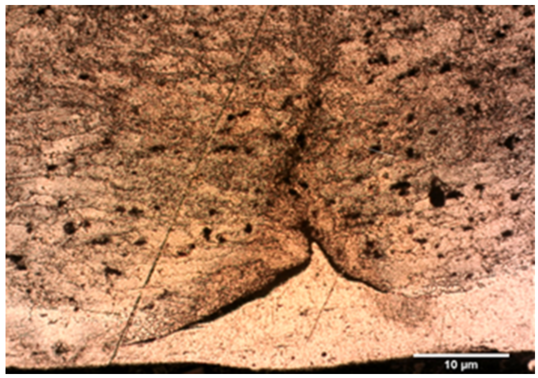

Figure 6. Remnants of joint line at the bottom of the FSW joint for a tapered cylinder pin.

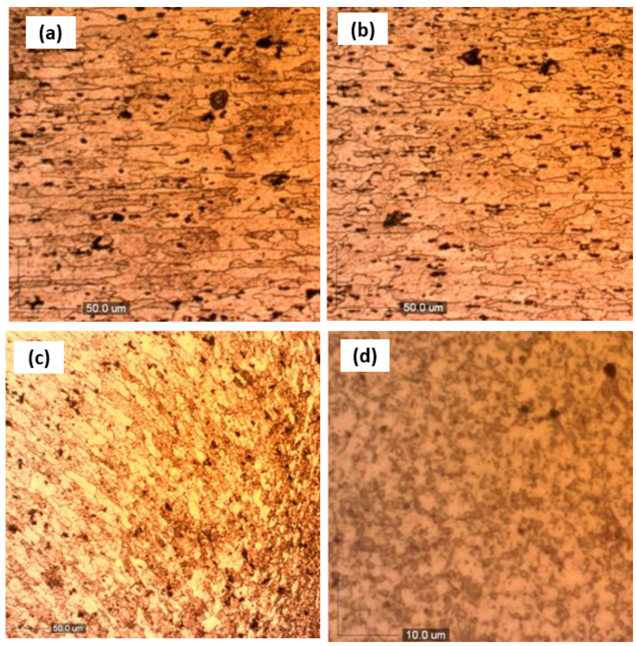

Figure 7. Grain morphology at 50 $\times$ magnification of **(a)** parent material, **(b)** HAZ, **(c)** TMAZ, and **(d)** NZ.

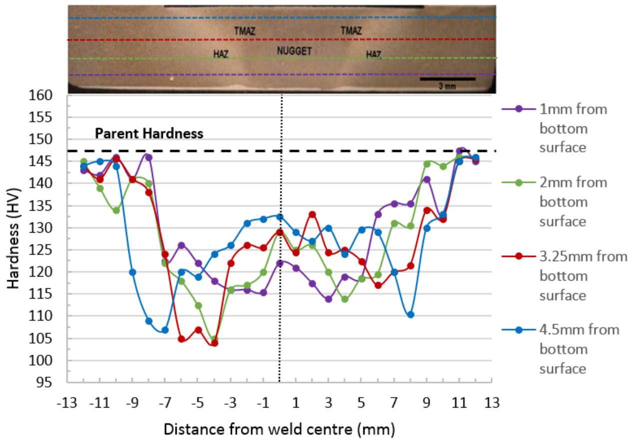

Figure 8. Tapered cylinder pin – hardness data at different heights in the weld thickness.

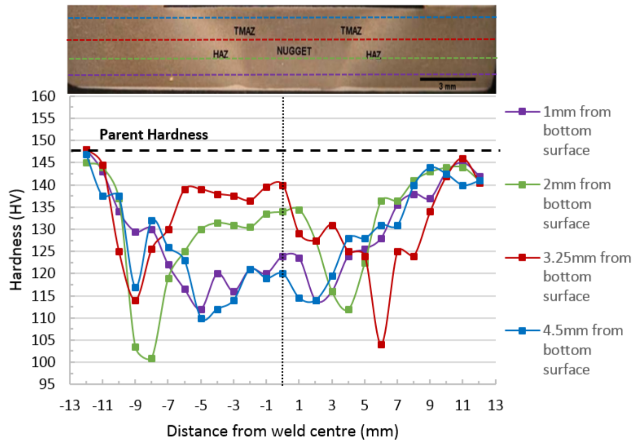

Figure 9. Square pin – hardness data at different heights in the weld thickness.

is typical of the alloy, which has temper designation T3 (solution heat treated, cold worked, and naturally aged). Figure 7b shows the microstructure of the HAZ. The HAZ and parent material were found to have similar microstructures as no deformational action from the tool is felt in this zone. There is insufficient evidence from the microstructure to suggest that recrystallization took place. Figure 7c shows the plastically strained microstructure of the TMAZ. This was due to plastic strain induced by the mechanical action of the tool. Average grain size in the TMAZ was found to be similar to the parent material however a wider range of grain size was apparent throughout the TMAZ. Figure 7c shows the fine equiaxed grain structure of the NZ.

The grain morphologies found in the various weld zones were qualitatively similar regardless of the pin used. Grain size in the NZ seemed to vary slightly as a result of pin profile (Table 1). The average grain size in the NZ for the square, tapered cylinder and triflute pins was calculated as 2.19, 2.3 and 2.23 µm, respectively. The differences in NZ grain size may have been as a result of the increased plastic deformation and stirring generated by the flutes in the triflute design and the flat faces of the square pin design.

Figures 8–10 show the measured hardness values recorded on the grid for the three tools in question. The measured hardness across each of the weld zones is below that of the parent material. This suggests that the strength of the weld will be lower than the parent material strength.

In all cases, hardness decreased from the parent material into the HAZ and increased from the HAZ, through the TMAZ, into the NZ. Hence, it is clear that the material in the HAZ experienced softening due to the process, even though changes in microstructure from the parent material to the HAZ were not apparent from the post mortem microstructure characterisation. Relatively constant hardness is found across the NZ.

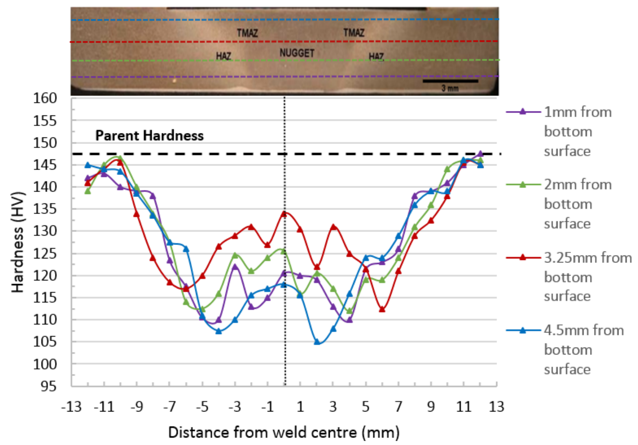

Figure 10. Triflute pin – hardness data at different heights in the weld thickness.

4 Conclusions

Flat plates of AA2024-T3 (4.8 mm thick) were butt welded using Friction Stir Welding. Three pairs of plates were welded under the same operating conditions but with differing pin profiles. The pin profiles used were tapered cylindrical, square and tri-flute. A scroll shoulder element was used for each case.

In summary, the main conclusions drawn from this work are:

1. The combined analyses of microstructure and microhardness showed a zonal transition from the unaffected parent material to a HAZ, a TMAZ, and a NZ in the centre of the weld.

2. Measured hardness varied through each FSW zone. The hardness in each zone was below that of the parent material.

3. The HAZ had the lowest hardness across the weld profile for each pin type tested. A lower hardness in this area could be due to either recovery (reduction in dislocation density) or recrystallization of the grains. Based on the evidence provided is difficult to confirm if recrystallization took place.

4. The cylindrical pin produced a tunnel defect and showed remnants of the joint line due to a lack of plastic deformation. Pin profiles with flat surface features and/or flutes produced a consolidated joint and are recommended over the tapered cylinder pin for future work.

Edited by: G. Hao
Reviewed by: E. Ahearne and another anonymous referee

References

Flores, O. V., Kennedy, C., Murr, L. E., Brown, D., and Pappu, S.: Microstructural issues in a Friction-Stir-Welded Aluminum Alloy, Scripta Mater., 38, 703–708, 1998.

Mishra, R. S. and Ma, Z. Y.: Friction stir welding and processing, Mater. Sci. Eng. R Rep., 50, 1–78, 2005.

Thomas, W. M.: Friction-stir butt welding, GB Patent No. 9125978.8, International patent application No. PCT/GB92/02203, 1991.

Trimble, D., Monaghan, J., and O'Donnell, G. E.: Force generation during friction stir welding of AA2024-T3, CIRP Ann. – Manufact. Technol., 61, 9–12, 2012.

Xiaocong, H., Fengshou, G., and Ball, A.: A review of numerical analysis of friction stir Welding, Prog. Mater. Sci., 65, 1–66, 2014.

Yang, Y., Kalya, P., Landers, R. G., and Krishnamurthy, K.: Automatic gap detection in friction stir butt welding operations, Int. J. Mach. Tools Manufact., 48, 1161–1169, 2008.